A germ-line *Tsc1* mutation causes tumor development and embryonic lethality that are similar, but not identical to, those caused by *Tsc2* mutation in mice

Toshiyuki Kobayashi*, Osamu Minowa†, Yoshinobu Sugitani†, Setsuo Takai‡, Hiroaki Mitani*, Etsuko Kobayashi*, Tetsuo Noda†§, and Okio Hino*‖

Departments of *Experimental Pathology and †Cell Biology, Cancer Institute, Japanese Foundation for Cancer Research, 1-37-1 Kami-ikebukuro, Toshima-ku, Tokyo 170-8455, Japan; ‡Department of Clinical Radiology, Faculty of Health Sciences, Hiroshima International University, Kurose-cho, Hiroshima 724-0695, Japan; and §Department of Molecular Genetics, Tohoku University School of Medicine, 2-1 Seiryo-machi, Aoba-ku, Sendai 980-8575, Japan

Edited by Bert Vogelstein, Johns Hopkins Oncology Center, Baltimore, MD, and approved May 23, 2001 (received for review January 22, 2001)

Tuberous sclerosis (TS) is characterized by the development of hamartomas in various organs and is caused by a germ-line mutation in either *TSC1* or *TSC2* tumor suppressor genes. From the symptomatic resemblance among TS patients, involvement of TSC1 and TSC2 products in a common pathway has been suggested. Here, to analyze the function of the Tsc1 product, we established a line of *Tsc1* (*TSC1* homologue) knockout mouse by gene targeting. Heterozygous *Tsc1* mutant (*Tsc1*$^{+/-}$) mice developed renal and extra-renal tumors such as hepatic hemangiomas. In these tumors, loss of wild-type *Tsc1* allele was observed. Homozygous *Tsc1* mutants died around embryonic days 10.5–11.5, frequently associated with neural tube unclosure. As a whole, phenotypes of *Tsc1* knockout mice resembled those of *Tsc2* knockout mice previously reported, suggesting that the presumptive common pathway for Tsc1 and Tsc2 products may also exist in mice. Notably, however, development of renal tumors in *Tsc1*$^{+/-}$ mice was apparently slower than that in *Tsc2*$^{+/-}$ mice. The *Tsc1* knockout mouse described here will be a useful model to elucidate the function of Tsc1 and Tsc2 products as well as pathogenesis of TS.

Tuberous sclerosis (TS) is an autosomal dominantly inherited disease characterized by the development of hamartomas and benign tumors in various organs such as brain, kidney, and heart (1). A germ-line mutation in either *TSC1* or *TSC2* genes (2, 3), both of which act as tumor suppressors (4, 5), is a genetic factor responsible for pathogenesis of TS. The similar symptoms of TS patients associated with *TSC1* or *TSC2* mutations suggest that the products of *TSC1* and *TSC2* are involved in a common physiological pathway (1, 6). *TSC1* encodes a protein with a molecular mass of ≈130 kDa, hamartin, which contains a coiled-coil domain in the carboxyl-terminal half (3). *TSC2* encodes tuberin, a rap1-GTPase activating protein homology domain-containing protein with a molecular mass of ≈180 kDa (2). Although several studies concerned with functions of these products have been reported, *in vivo* functions of them remain to be elucidated (1, 7, 8).

The tumor suppressor function of *TSC2* became evident by studies of rodents with a germ-line *Tsc2* mutation such as the Eker rat (9–13) and *Tsc2* knockout mice (14, 15). Both heterozygous *Tsc2* mutant rats and mice develop hereditary renal tumors and extra-renal tumors carrying a second hit of *Tsc2* gene (14–17). Homozygosity of *Tsc2* mutation leads to the embryonic lethality both in rats (9, 18) and mice (15, 16), indicating that the function of tuberin is essential for mammalian development.

We also isolated a rat homologue of *TSC1* (*Tsc1*) and analyzed its mutation in chemically induced renal tumors in wild-type rats, in which *Tsc2* mutations were found with high frequency (≈50%) (19). In those tumors, we found *Tsc1* mutations in a case with no *Tsc2* mutation (19). These results suggest that mutations of *Tsc1* and *Tsc2* are involved in the development of chemically induced renal tumors in rats, although the latter is more common. These systems of renal tumorigenesis could be an experimental approach to analyze the function of Tsc1 and its relationship with function of Tsc2 *in vivo*. However, the rat or mouse model carrying the germ-line *Tsc1* mutation, which should be essential for precise analysis to elucidate the molecular mechanism of pathogenesis of TS, is not yet available. Therefore, in this study, we generated *Tsc1* mutant mice by gene targeting and initially characterized its phenotypes about tumor development and embryonic lethality.

Materials and Methods

Genomic DNA Cloning and cDNA Amplification. A mouse embryonic stem (ES) cell (clone J1, 129/Sv background) genomic DNA library was screened with rat *Tsc1* cDNA (19) as a probe, and a positive clone (λMTSC1) was isolated and analyzed by restriction enzyme digestion and sequencing. The numbering of exons in this study followed those of human and rat *Tsc1* genes (3, 19). Mouse *Tsc1* cDNA fragments corresponding to the coding region of rat and human counterparts were amplified by reverse transcription-PCR using total RNA from ES cells as a template. The 5′ half was amplified with a primer set, MTRTF1 (5′-AGCATAATTGAGTGAGAGAATG-3′) and MTRTR2 (CCATGCACACAGTCATCTTG-3′). The 3′ half was amplified with a primer set, MTRTF2 (5′-CAAGATGACTGTGTGCATGG-3′) and MTRTR1 (5′-ACACTGACAGACCCTCTTCA-3′). MTRTF1 and MTRTR1 were designed from the rat *Tsc1* cDNA sequence in expectation of high homology between rat and mouse. In the above sequences, the positions of putative initiation (in MTRTF1) and termination (in MTRTR1, complementary strand) codons for translation are underlined. MTRTF2 and MTRTR2 were sequences in exon 12 found in λMTSC1. Amplified products were directly sequenced for both strands by primer walking.

Fluorescence *in Situ* Hybridization. For fluorescence *in situ* hybridization, the insert DNA of λMTSC1 was used as a probe. Mouse pro-metaphase chromosomes were prepared from embryonic fibroblasts in early passages by standard technique. The proce-

This paper was submitted directly (Track II) to the PNAS office.

Abbreviations: TS, tuberous sclerosis; E, embryonic day; ES, embryonic stem; IRES, internal ribosome entry site; EGFP, enhanced green fluorescent protein; ENU, *N*-ethyl-*N*-nitrosourea; HE, hematoxylin and eosin; LOH, loss of heterozygosity.

Data deposition: The sequence reported in this paper has been deposited in the GenBank database (accession no. AB047561).

‖To whom reprint requests should be addressed. E-mail: ohino@ims.u-tokyo.ac.jp.

The publication costs of this article were defrayed in part by page charge payment. This article must therefore be hereby marked "*advertisement*" in accordance with 18 U.S.C. §1734 solely to indicate this fact.

www.pnas.org/cgi/doi/10.1073/pnas.151033798

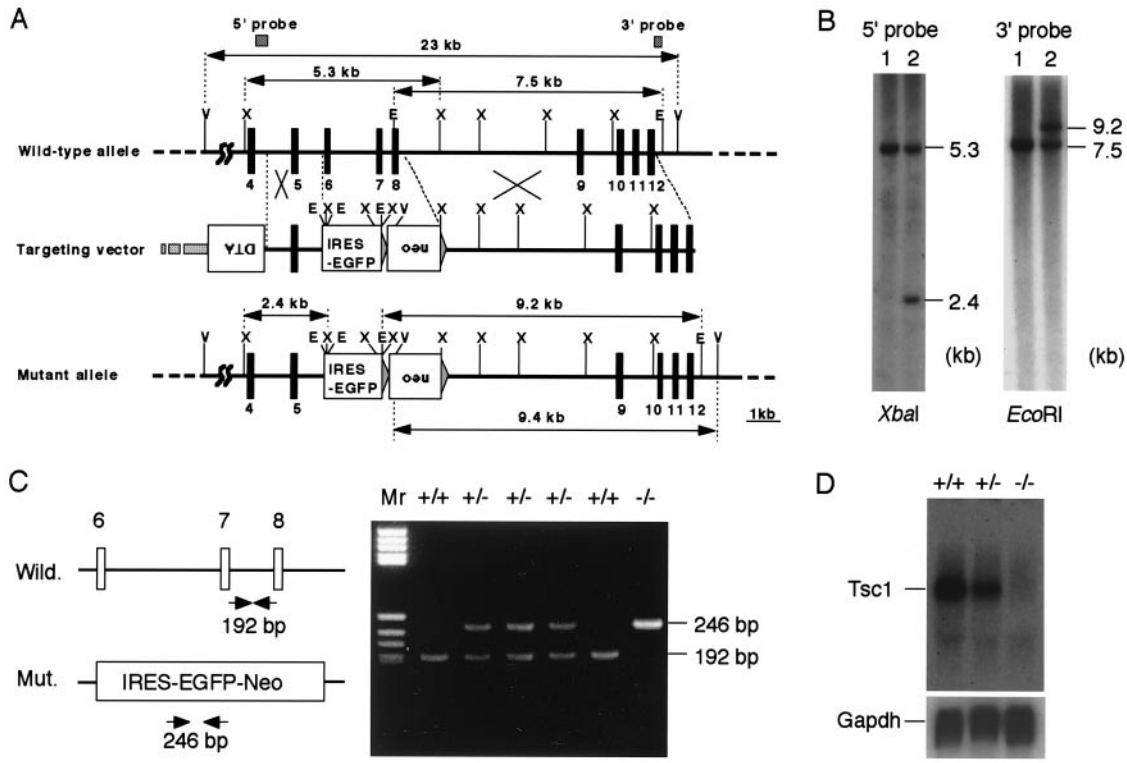

Fig. 1. Inactivation of mouse *Tsc1* gene. (*A*) Structure of targeting vector and wild-type and mutant alleles. Exons are denoted with filled boxes with numbers, and restriction enzyme sites (E, *Eco*RI; V, *Eco*RV; X, *Xba*I) are shown. Expression cassettes for the neomycin resistance gene (neo) and diphtheria toxin A-chain gene (DTA), and the coding sequence for EGFP preceded with an IRES (IRES-EGFP) are shown as open boxes. Length (kb) of restriction fragments and positions of probes (5′ and 3′ probes) used for genotyping are denoted by arrows and hatched boxes, respectively. (*B*) Southern blot analysis of ES cells. *Xba*I- or *Eco*RI-digested DNAs from homologous recombinant (lane 2) and control (lane 1) ES cells were probed with probes shown in *A*. Sizes (kb) of bands are shown. (*C*) PCR genotyping of F2 embryos. (*Left*) Schematic representation of primers and product size (bp). (*Right*) A representative result of PCR genotyping of E10.0 embryos obtained by double heterozygous breeding. Wild-type (+/+), heterozygous (+/−), and homozygous mutant (−/−) embryos were present in this litter. (*D*) Northern blot analysis of E11.0 embryos. (*Upper*) The expression profile of *Tsc1* mRNA (≈8.0 kb) in wild-type (+/+), heterozygous (+/−), and homozygous mutant (−/−) embryos. Probe used was a *Tsc1* cDNA fragment covering the 3′ region downstream from exon 8. (*Lower*) The result with a *GAPDH* cDNA probe using the same blot.

dures of fluorescence *in situ* hybridization and microscopic observation were carried out as described (20).

Construction of a Targeting Vector and Gene Targeting. For the construction of a targeting vector, pBmTsc1-KO, a 1.8-kb genomic DNA fragment from a *Bam*HI site in intron 4 to the splicing acceptor site in intron 5 and an 8-kb fragment from an *Apa*I site in intron 8 to a *Bam*HI site in intron 12 were used as 5′ and 3′ homologous regions, respectively. A DNA fragment containing internal ribosome entry site (IRES) of the encephalomyocarditis virus (21), enhanced green fluorescent protein (EGFP)-coding sequence (CLONTECH) followed by a poly(A) addition signal (pA), was introduced between 5′ and 3′ homologous regions to delete exons 6 to 8. IRES-EGFP-pA was inserted just after the splicing acceptor of intron 5, allowing a splicing event between exon 5 and IRES and the expression of EGFP to occur. At the 3′ end of this IRES-EGFP-pA unit, an expression cassette of neomycin resistance gene (neo) was introduced in opposite orientation. The diphtheria toxin A-chain expression cassette was used for negative selection (22). For gene targeting, linearized pBmTsc1-KO was introduced into J1 ES cells by electroporation. Subsequent cloning of homologous recombinant clones and production of chimera mice were carried out as described (23). F_1 mice were

Table 1. Genotype analysis of embryos obtained by double heterozygous breedings

			Genotype of *Tsc1*				
Embryonic day	Litters	Total number	+/+	+/−	−/−	Resorbed†	*Tsc2*$^{-/-}$‡ embryos
E9.0∼9.5	2	21	5	10	6 (1)*	0	19 (7)*
E10.0∼10.5	6	52	13	25	12 (4)	2	10 (5)
E11.0∼11.5	7	63	17	32	12 (7)§	2	17 (15)§
E12.0∼12.5	5	43	12	20	8 (7)	3	6 (5)
E13.0∼13.5	4	38	9	18	7 (7)	4	1 (1)

*The number in parentheses indicates the number of dead embryos among total −/− embryos.
†Number of resorbed embryos could not be genotyped.
‡Data from ref. 14 for comparison.
§Survival rates did not show the significant difference ($P = 0.092$) by Fisher's exact test.

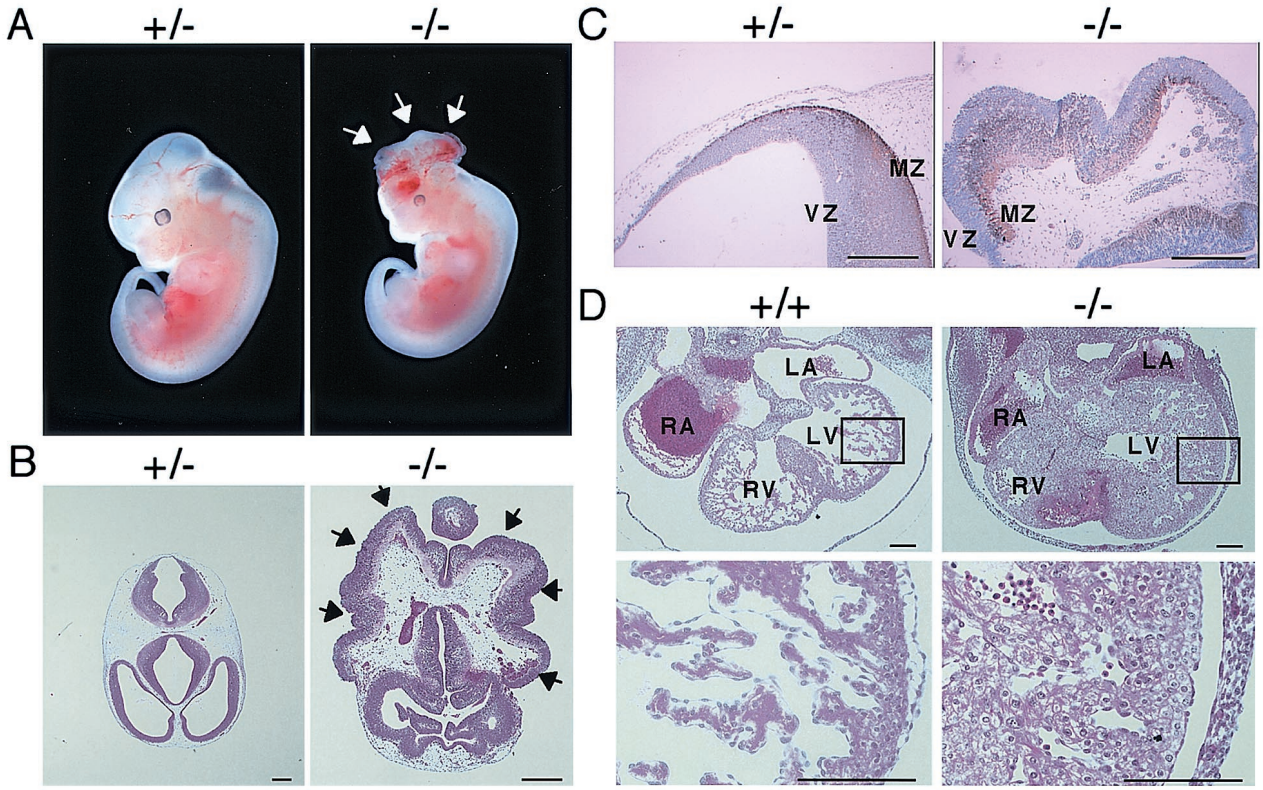

Fig. 2. Analysis of homozygous *Tsc1* mutant embryos. (*A*) Macroscopic appearance of heterozygous (+/−) and homozygous *Tsc1* mutant (−/−) embryos at E12.0 with heartbeat. Arrows point to the unclosed neural tube exhibiting exencephaly. (*B*) Histology of head region of heterozygous (+/−) and homozygous (−/−) mutant embryos at E12.0 with heartbeat shown by HE staining. Field of homozygous mutant is enlarged with twice the magnitude of that of the heterozygous mutant. Arrows point to the unclosed region of the neural fold exposed to the outside. (*C*) Immunostaining of neural tube with anti-class III β-tubulin antibody (TuJ1). Sections of the head region from heterozygous (+/−) and homozygous (−/−) mutant embryos at E12.0 with heartbeat were stained with TuJ1. After immunostaining, a counterstain with HE was performed. Positive signals were seen as brown staining. VZ, ventricular zone; MZ, marginal zone. (*D*) Histological analysis of heart from wild-type (+/+) and homozygous *Tsc1* mutant (−/−) embryos at E12.0 with heartbeat shown by HE staining. (*Lower*) Enlarged view of the region enclosed with a rectangle in the upper panel. LA, left atrium; LV, left ventricle; RA, right atrium; RV, right ventricle. (Scale bars: *B* and *C* = 200 μm; *D* = 100 μm.)

obtained by crossing male chimera mice with female C57BL/6J mice.

Southern and Northern Blot Analyses and PCR Genotyping. For genotyping by Southern blot analysis, *Xba*I-digested DNAs were hybridized with 5′ outside probe (0.5-kb *Cla*I–*Bam*HI fragment), and *Eco*RI- or *Eco*RV-digested DNAs were hybridized with 3′ outside probe (0.3-kb *Bam*HI–*Eco*RI fragment). Genotyping by PCR was performed with the following primers: INT7F1 (5′-TCTGAGTCCGAGTCAAGAGT-3′ in intron 7) and INT7R1 (5′-TAGATGTGAAGTTGTGTGGCA-3′ in intron 7) for wild-type allele; and EGFPF2 (5′-CATGGACGAGCTGTACAAGT-3′ in EGFP coding sequence) and EGFPR2 (5′-GGACAAACCACAACTAGAATG-3′ in EGFP coding sequence) for mutant allele. Conditions of PCR were essentially the same as described (13). Northern blot analysis was carried out as described (11).

Table 2. Development of macroscopic renal tumors in *Tsc1*$^{+/-}$ mice

Age (months)	*Tsc1*$^{+/-}$*	*Tsc2*$^{+/-}$*†
9~12	*n* = 5	*n* = 9
Mice with unilateral tumors	0	2
Mice with bilateral tumors	0	7
Tumor multiplicity (/kidney)‡	—	2.3 ± 0.3
Diameter of tumor (mm)‡	—	0.8 ± 0.1
15~18	*n* = 14	*n* = 8
Mice with unilateral tumors	4	0
Mice with bilateral tumors	5	8
Tumor multiplicity (/kidney)‡	1.7 ± 0.3§	5.5 ± 0.6§
Diameter of tumor (mm)‡	1.0 ± 0.1	1.1 ± 0.2

*All of examined mice were F1 on a hybrid 129/SvJ-C57BL6/J background.
†Data from our previous study (ref. 14) for comparison.
‡Multiplicity and diameter of tumor were of tumor-bearing kidneys (mean ± SEM).
§$P < 0.0001$ by Mann–Whitney test.

***N*-Ethyl-*N*-Nitrosourea (ENU) Treatment.** F_1 male *Tsc1*$^{+/-}$ mice were crossed with female C57BL/6J mice, and ENU solution was i.p. injected (50 mg/kg body weight) into the pregnant mother mice at embryonic day (E) 15.0 (noon of the day on which a vaginal plug was detected was defined as E0.5). Offspring were killed at 11 weeks of age for histological analyses.

Histological Analyses. Tissues from mice or embryos were fixed in either 10% buffered formaline or Bouin's fixative. Dehydration, embedding in paraffin, sectioning, and staining with hematoxylin and eosin (HE) were performed by standard protocols. Immunostaining with anti-β-tubulin III (clone TuJ1; Babco, Richmond, CA) was performed as described by using VECTASTAIN ABC horseradish peroxidase kit (Vector Laboratories) (13).

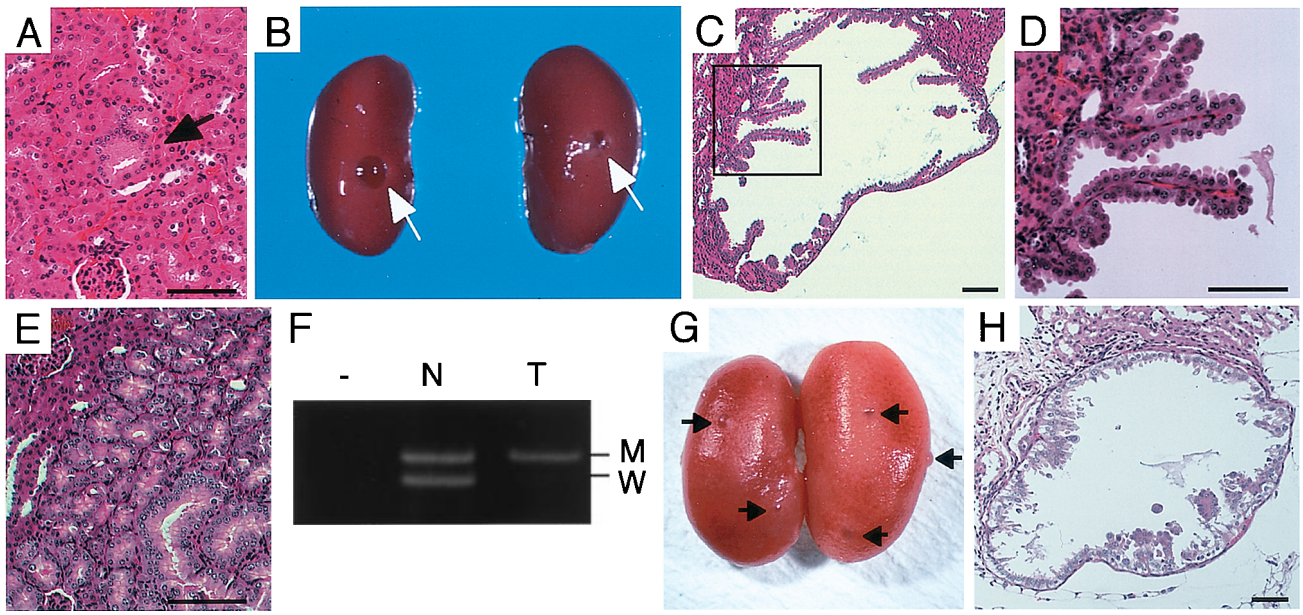

Fig. 3. Renal tumors in *Tsc1*$^{+/-}$ mice. (*A*) A phenotypically altered renal tubule (arrow) shown by HE staining. (*B*) Macroscopic renal cysts (arrows) developed in a 15-month-old mouse. (*C* and *D*) Histology of a renal cystadenoma shown by HE staining. *D* is an enlarged view of region enclosed with a rectangle in *C*. (*E*) Histology of a renal adenoma exhibiting tubular structure shown by HE staining. (*F*) Loss of wild-type *Tsc1* allele in a renal tumor of *Tsc1*$^{+/-}$ mice. Representative result of LOH analysis is shown. Lanes T, tumor; N, normal counterpart; −, no input DNA sample. Products from mutant allele (M, 220 bp) and from wild-type allele (W, 192 bp) are indicated. (*G*) Macroscopic renal cysts (arrows) developed in an 11-week-old mouse transplacentally treated with ENU. (*H*) Histology of a renal cystadenoma developed by ENU treatment shown by HE staining. (Scale bars = 50 μm.)

Loss of Heterozygosity (LOH) Analysis. DNA samples from formaline-fixed, paraffin-embedded tissues were prepared as described (13). Primers used for LOH analysis were INT7F1 and INT7R1 for wild-type allele and NEOF1 (5′-GGCTGCTATTGGGCGAAGT-3′ in neo cassette) and NEOR1 (5′-CCTGATGCTCTTCGTCCAG-3′ in neo cassette) for mutated allele. Conditions of PCR were essentially the same as described (13).

Results and Discussion

Cloning and Gene Targeting of Mouse *Tsc1*. To obtain the structural information about mouse hamartin, mouse *Tsc1* cDNA fragments were amplified by reverse transcription-PCR (see *Materials and Methods*). The mouse *Tsc1* cDNA sequence corresponding to the coding region of rat and human counterparts encoded 1,160 aa residues showing ≈87% and ≈95% identities with human and rat hamartins, respectively (data not shown, GenBank accession no. AB047561) (3, 16). By Northern blot analysis, a major ≈8.0-kb mRNA of *Tsc1* was detected in brain, heart, kidney, heart, liver, and embryos at E9.5 to E13.5 (data not shown). Also, we isolated a phage genomic DNA clone (λMTSC1) covering exons 4–12 of mouse *Tsc1* gene (Fig. 1*A*). By fluorescence *in situ* hybridization, *Tsc1* gene appeared to be localized on mouse chromosome 2, band B-C1.1 (data not shown). Recently, Cheadle *et al.* (24) reported the genomic organization and comparative analysis of the mouse *Tsc1*. An alanine residue at position 381 of predicted mouse hamartin sequence in their report was missed in our sequence, probably because of a difference in the usage of splicing acceptor at the 3′ end of intron 11 (data not shown).

To disrupt *Tsc1*, a targeting vector (pBmTsc1-KO), in which exons 6–8 were replaced by IRES-EGFP-pA expression unit and a neo-expression cassette, was constructed and used for gene targeting in ES cells (Fig. 1*A*). These deleted exons encode a part of the highly conserved region between mammalian and fly *Tsc1* homologues that may be functionally important (7, 8). Skipping these three exons, splicing from exon 5 to exon 9 should result in frameshift. Male germ-line chimeras were obtained using a correctly targeted ES cell clone, and F_1 mice were obtained by crossing of those chimeras with C57BL/6J female mice (Fig. 1*B*). F_1 mice heterozygous for *Tsc1* mutation (*Tsc1*$^{+/-}$) were born and grew with normal appearance. Northern blot analysis of E11.0 embryos obtained by double heterozygous breeding revealed that ≈8.0-kb mRNA of *Tsc1* disappeared in homozygous mutant (*Tsc1*$^{-/-}$) embryos (Fig. 1 *C* and *D*).

Embryonic Lethality of Homozygous *Tsc1* Mutants. *Tsc1*$^{-/-}$ mice were not obtained by F_1 double heterozygous breedings (32 wild-type and 62 *Tsc1*$^{+/-}$ mice among 94 F_2 mice at birth). Analysis of embryos revealed that most of *Tsc1*$^{-/-}$ embryos died between E10.5 and E11.5 (Table 1). This stage for lethality is similar to that of *Tsc2*-deficient embryos, although more embryos alive at E11.0 to E12.5 were found in the *Tsc1* case (30% of *Tsc1*$^{-/-}$ embryos versus 13% of *Tsc2*$^{-/-}$ ones; refs. 14 and 15). Typically, *Tsc1*$^{-/-}$ embryos alive at E9.0-E12.5 were smaller than control embryos, and about one-third (6 of 19) exhibited neural tube unclosure at the head region (Fig. 2 *A* and *B*). Histologically, the neural tube of those embryos exhibited a disorganized architecture, although they were positive for β-tubulin III, a neuronal differentiation marker, suggesting the differentiation of neural lineage in them (Fig. 2*C*). Hearts of some *Tsc1*$^{-/-}$ embryos exhibited abnormal morphology of myocardial cells (Fig. 2*D*). Although hypoplastic appearance of livers was noticed in *Tsc1*$^{-/-}$ embryos as reported in *Tsc2*$^{-/-}$ embryos (data not shown, ref. 15), the *Tsc1*$^{-/-}$ embryos were much smaller than the control ones; therefore, developmental delay and hypoplasia of livers in those embryos should be carefully analyzed further. Nonetheless, phenotypic similarities found between *Tsc1*- and *Tsc2*-deficient embryos suggest that, during the mouse embryonic development, hamartin and tuberin may function in a common pathway.

Development of Renal Tumors in Heterozygous *Tsc1* Mutant Mice. *Tsc2*$^{+/-}$ mice develop macroscopically visible renal carcinomas and/or renal cystadenomas by the age of 10 months in all cases

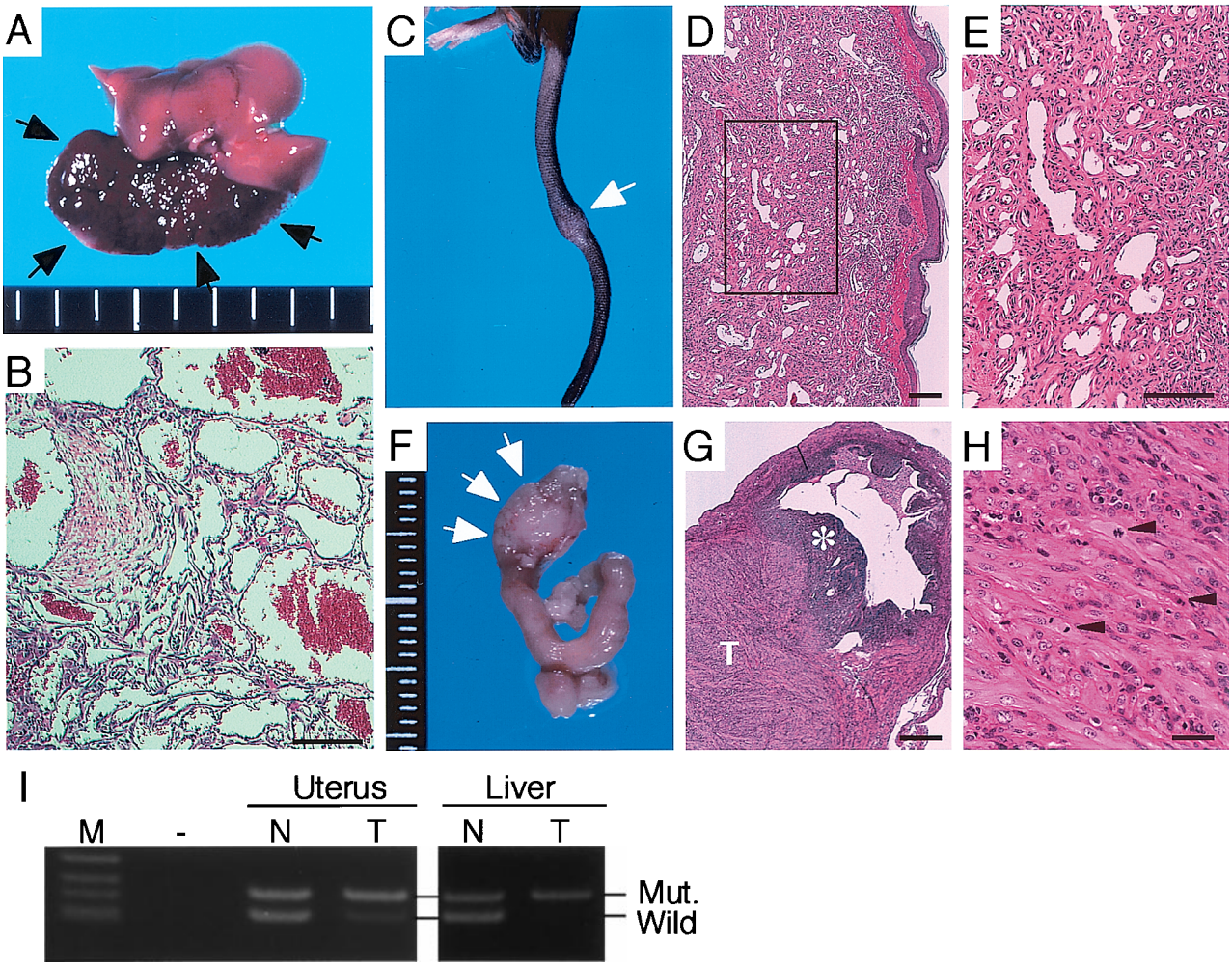

Fig. 4. Extra-renal tumors in *Tsc1*$^{+/-}$ mice. (*A*) Macroscopic view of a hepatic hemangioma (arrows) developed in a 17-month-old mouse. (*B*) Histology of a hepatic hemangioma shown by HE staining. (*C*) Macroscopic view of a tail of 15-month-old mouse showing a knob (arrow). (*D* and *E*) Histology of a hemangioma developed in the knob in *C* shown by HE staining. *E* is an enlarged view of the region enclosed with a rectangle in *D*. (*F*) Macroscopic view of a uterus leiomyoma/leiomyosarcoma developed in a 16-month-old mouse (arrows). (*G and H*) Histology of the leiomyoma/leiomyosarcoma in *F* shown by HE staining. In *G*, * and T indicate the endometrium and tumor region, respectively. Arrowheads in *H* point to mitotic cells. (*I*) Loss of wild-type *Tsc1* allele in extra-renal tumor of *Tsc1*$^{+/-}$ mice. Representative results of LOH analysis are shown. Lanes T, tumor; N, normal counterpart. M, size marker; −, no input DNA sample. Products from mutant allele (Mut., 220 bp) and from wild-type allele (Wild, 192 bp) are indicated. (Scale bars: *B*, *D*, *E*, and *G* = 100 μm; H = 10 μm.)

(14, 15). In addition, hepatic hemangiomas and other tumors in extremities developed in *Tsc2*$^{+/-}$ mice with a high frequency (14, 15). We also observed tumor development in F_1 *Tsc1*$^{+/-}$ mice. At 9–12 months of age, although macroscopic tumors were not observed, phenotypically altered tubules, the preneoplastic lesions of renal carcinogenesis, were found in kidney sections from *Tsc1*$^{+/-}$ mice (n = 5) (Table 2 and Fig. 3*A*). At least one phenotypically altered tubule was observed in the largest dorsoventral section from each kidney. By the age of 15–18 months, small cysts with a diameter of 0.5–2.0 mm appeared on the surface of kidneys in *Tsc1*$^{+/-}$ mice (9 of 14 = 64%) (Table 2 and Fig. 3*B*). Histologically, these cysts were similar to those developed in *Tsc2*$^{+/-}$ mice, showing papillary neoplastic outgrowth into the lumen (Fig. 3 *C* and *D*) (14, 15). In addition to cystic lesions, there were tumors exhibiting tubular structure (Fig. 3*E*). Using DNA samples from microdissected specimens, we examined the LOH at the *Tsc1* locus in renal tumors by PCR (Fig. 3*F* and data not shown). Of six available cases examined, two cases clearly showed the loss of wild-type *Tsc1* allele, which suggests that a second hit of *Tsc1* may be a critical event for the development of renal tumors in *Tsc1*$^{+/-}$ mice. As an attempt to accelerate renal carcinogenesis in *Tsc1*$^{+/-}$ mice, we performed transplacental administration of ENU (25) as in our previous study for *Tsc2* knockout mice (14). Of 13 *Tsc1*$^{+/-}$ mice treated with ENU, six mice developed bilateral macroscopic cysts in kidneys by 11 weeks of age (Fig. 3*G*). These cysts had a diameter less than 1.5 mm and showed similar histological features to those developed in ENU-treated *Tsc2*$^{+/-}$ mice (Fig. 3*H*) (14). Although kidneys from the other seven ENU-treated *Tsc1*$^{+/-}$ mice did not show macroscopic cysts, microscopic phenotypically altered tubules and adenomatous lesions were observed in the cortex region (data not shown). None of the kidney sections from ENU-treated wild-type mice (n = 6) showed such renal lesions. Thus, transplacental ENU treatment accelerated renal tumorigenesis in *Tsc1*$^{+/-}$ mice. To confirm that a second hit in the wild-type *Tsc1* allele is induced by ENU, mutational analysis of *Tsc1* in these ENU-accelerated renal tumors is to be desired. Such analysis will be useful to analyze the mutation spectrum of *Tsc1* for comparison with that of human *TSC1* (1).

Results obtained in this study indicate that a germ-line *Tsc1* mutation causes renal tumorigenesis in mice as a *Tsc2* mutation. However, spontaneous development of macroscopic renal tu-

mors was apparently slower in $Tsc1^{+/-}$ mice, compared with $Tsc2^{+/-}$ mice on the same genetic background (C57BL6/J:129/Sv; Table 2, ref. 14). Although the molecular mechanism underlying this difference is currently unknown, it may be relevant to the difference in frequencies of second hit or in functions of gene products. In the case of human, there is a debate about the symptomatic difference between TS patients associated with *TSC1* and *TSC2* mutations (1). Dabora *et al.* (26) provided evidence for the increased severity of *TSC2*-associated patients than *TSC1*-associated ones. Elucidation of the molecular basis for the differences of renal tumorigenesis found here may provide some important clues for the understanding of pathogenesis of human TS. Nonetheless, development of renal tumors and extra-renal tumors (see below) in both $Tsc1^{+/-}$ and $Tsc2^{+/-}$ mice suggests that tuberin and hamartin have a functional relationship for tumor suppression.

Development of Extra-Renal Tumors in Heterozygous *Tsc1* Mutant Mice. Macroscopic hemangiomas in liver also were developed in $Tsc1^{+/-}$ mice by 15–18 months of age (10 of 14 = 71%) (Fig. 4*A*). This incidence of hepatic hemangiomas resembled that of $Tsc2^{+/-}$ mice at a similar age (≈80%) (14). Histologically, these hemangiomas could be classified as cavernous hemangiomas and resembled those developed in $Tsc2^{+/-}$ mice (Fig. 4*B*) (14, 15). Although there was no higher incidence of mortality in $Tsc1^{+/-}$ mice compared with wild-type mice during observation of 18 months, we noticed sudden death of $Tsc1^{+/-}$ mice older than 18 months of age, probably as a result of the rupture of huge hepatic hemangiomas (unpublished observation). In addition, we found a hemangioma in the tail and a leiomyoma/leiomyosarcoma in the uterus (Fig. 4 *C–H*). Also in $Tsc2^{+/-}$ mice, hemangiomas/hemangiosarcomas in the extremities were often (≈10%) developed by the age of 18 months (ref. 15 and unpublished observation). Although uterus tumors are rare in mice, $Tsc2^{+/-}$ Eker rat females frequently develop leiomyomas/leiomyosarcomas (27). None of these extra-renal tumors was observed in wild-type mice analyzed as a control in this study (n = 15). We examined LOH of *Tsc1* in those extra-renal tumors by PCR (Fig. 4*I*). Of three hepatic hemangiomas examined, one case clearly showed the loss of wild-type *Tsc1* allele. The uterine leiomyoma/leiomyosarcoma also showed the loss of wild-type *Tsc1* allele. These LOHs suggest that a second hit of *Tsc1* may be a critical event for the development of these extra-renal tumors in $Tsc1^{+/-}$ mice. Together, these results indicate that, in mice, a germ-line *Tsc1* mutation contributes to the development of extra-renal tumors as a germ-line *Tsc2* mutation.

In this study, similarities of phenotypes between *Tsc1* and *Tsc2* knockout mice were revealed for both tumor development and embryonic lethality, although some differences were also observed. As a whole, these phenotypical similarities must reflect the involvement of hamartin and tuberin in a common pathway, as has been suggested from the symptom of TS patients. Although phenotypes caused by *Tsc1* and *Tsc2* mutations in mice are different from those of human TS patients, involvement of hamartin and tuberin in a common pathway may be conserved in both species. Elucidation of this presumptive common pathway is important for the understanding of tumorigenesis in mice as well as pathogenesis of TS patients. In combination with the use of *Tsc2* knockout mouse, our *Tsc1* knockout mouse will be a useful experimental model to unravel the functions of hamartin and tuberin and to elucidate the mechanism of tumor development associated with *Tsc1* and *Tsc2* mutations.

We thank H. Yamanaka, M. Miyagawa, T. Fukuda, and Y. Hirayama for technical assistance; H. Akazawa, I. Komuro, and H. Takeshima for helpful discussions; I. Ishikawa for plasmid preparation; and H. Sugano, T. Kitagawa, and A. G. Knudson for encouragement throughout this work. This work was supported in part by grants from the Ministry of Education, Science and Culture, the Ministry of Health and Welfare of Japan, the Program for Promotion of Fundamental Studies in Health Sciences of the Organization for Pharmaceutical Safety and Research, and the Program of Core Research for Evolutional Science and Technology of the Japan Science and Technology Corporation.

1. Cheadle, J. P., Reeve, M. P., Sampson, J. R. & Kwiatkowski, D. J. (2000) *Hum. Genet.* **107,** 97–114.
2. The European Chromosome 16 Tuberous Sclerosis Consortium (1993) *Cell* **75,** 1305–1315.
3. van Slegtenhorst, M., de Hoogt, R., Hermans, C., Nellist, M., Janssen, B., Verhoef, S., Lindhout, D., van den Ouweland, A., Halley, D., Young, J., *et al.* (1997) *Science* **277,** 805–808.
4. Green, A. J., Johnson, P. H. & Yates, J. R. W. (1994) *Hum. Mol. Genet.* **3,** 1833–1834.
5. Green, A. J., Smith, M. & Yates, J. R. W. (1994) *Nat. Genet.* **6,** 193–196.
6. van Slegtenhorst, M., Nellist, M., Nagelkerken, B., Cheadle, J., Shell, R., van den Ouweland, A., Reuser, A., Sampson, J., Halley, D. & van der Sluijs, P. (1998) *Hum. Mol. Genet.* **7,** 1053–1058.
7. Ito, N. & Rubin, G. M. (1999) *Cell* **96,** 529–539.
8. Lamb, R. F., Roy, C., Diefenbach, T. J., Vinters, H. V., Johnson, M. W., Jay, D. G. & Hall, A. (2000) *Nat. Cell Biol.* **2,** 281–287.
9. Hino, O., Klein-Szanto, A. J. P., Freed, J. J., Testa, J. R., Brown, D. Q., Vilensky, M., Yeung, R. S., Tartof, K. D. & Knudson, A. G. (1993) *Proc. Natl. Acad. Sci. USA* **90,** 327–331.
10. Hino, O., Kobayashi, T., Tsuchiya, H., Kikuchi, Y., Kobayashi, E., Mitani, H. & Hirayama, Y. (1994) *Biochem. Biophys. Res. Commun.* **203,** 1302–1308.
11. Kobayashi, T., Hirayama, Y., Kobayashi, E., Kubo, Y. & Hino, O. (1995) *Nat. Genet.* **9,** 70–74.
12. Yeung, R. S., Xiao, G.-H., Jin, F., Lee, W.-C., Testa, J. R. & Knudson, A. G. (1994) *Proc. Natl. Acad. Sci. USA* **91,** 11413–11416.
13. Kobayashi, T., Mitani, H., Takahashi, R., Hirabayashi, M., Ueda, M., Tamura, H. & Hino, O. (1997) *Proc. Natl. Acad. Sci. USA* **94,** 3990–3993.
14. Kobayashi, T., Minowa, O., Kuno, J., Mitani, H., Hino, O. & Noda, T. (1999) *Cancer Res.* **59,** 1206–1211.
15. Onda, H., Lueck, A., Marks, P. W., Warren, H. B. & Kwiatkowski, D. J. (1999) *J. Clin. Invest.* **104,** 687–695.
16. Kubo, Y., Mitani, H. & Hino, O. (1994) *Cancer Res.* **54,** 2633–2635.
17. Yeung, R. S., Xiao, G.-H., Everitt, J. I., Jin, F. & Walker, C. L. (1995) *Mol. Carcinog.* **14,** 28–36.
18. Rennebeck, G., Kleymenova, E. V., Anderson, R., Yeung, R. S., Artzt, K. & Walker, C. L. (1998) *Proc. Natl. Acad. Sci. USA* **95,** 15629–15634.
19. Satake, N., Kobayashi, T., Kobayashi, E., Izumi, K. & Hino, O. (1999) *Cancer Res.* **59,** 849–855.
20. Hagiwara, T., Tanaka, K., Takai, S., Maeno-Hikichi, Y., Mukainaka, Y. & Wada, K. (1996) *Genomics* **33,** 508–515.
21. Ghattas, I. R., Sanes, J. R. & Majors, J. E. (1991) *Mol. Cell. Biol.* **11,** 5848–5859.
22. Yagi, T., Ikawa, Y., Yoshida, K., Shigetani, Y., Takeda, N., Mabuchi, I., Yamamoto, T. & Aizawa, S. (1990) *Proc. Natl. Acad. Sci. USA* **87,** 9918–9922.
23. Nakai, S., Kawano, H., Yudate, T., Nishi, M., Kuno, J., Nagata, A., Jishage, K., Hamada, H., Fujii, H., Kawamura, K., *et al.* (1995) *Genes Dev.* **9,** 3109–3121.
24. Cheadle, J. P., Dobbie, L., Idziaszczyk, S., Hodges, A. K., Smith, A. J. H., Sampson, J. R. & Young, J. (2000) *Mamm. Genome* **11,** 1135–1138.
25. Hino, O., Mitani, H. & Knudson, A. G. (1993) *Cancer Res.* **53,** 5856–5858.
26. Dabora, S. L., Jozwiak, S., Franz, D. N., Roberts, P. S., Nieto, A., Chung, J., Choy, Y.-S., Reeve, M. P., Thiele, E., Egelhoff, J. C., *et al.* (2001) *Am. J. Hum. Genet.* **68,** 64–80.
27. Hino, O., Mitani, H., Katsuyama, H. & Kubo, Y. (1994) *Cancer Lett.* **83,** 117–121.